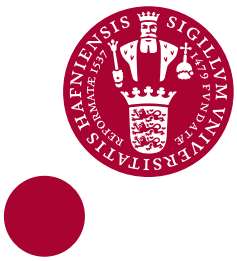

Computational Flux Balance Analysis Predicts that Stimulation of Energy Metabolism in Astrocytes and their Metabolic Interactions with Neurons Depend on Uptake of K(+) Rather than Glutamate

DiNuzzo, Mauro; Giove, Federico; Maraviglia, Bruno; Mangia, Silvia

Published in:
Neurochemical Research

DOI:
10.1007/s11064-016-2048-0

Publication date:
2017

Document version
Publisher's PDF, also known as Version of record

Neurochem Res (2017) 42:202–216
DOI 10.1007/s11064-016-2048-0

ORIGINAL PAPER

Computational Flux Balance Analysis Predicts that Stimulation of Energy Metabolism in Astrocytes and their Metabolic Interactions with Neurons Depend on Uptake of K^+ Rather than Glutamate

Mauro DiNuzzo[1] · **Federico Giove**[2,3] · **Bruno Maraviglia**[2,3] · **Silvia Mangia**[4]

Received: 1 June 2016 / Revised: 22 August 2016 / Accepted: 24 August 2016 / Published online: 14 September 2016

Abstract Brain activity involves essential functional and metabolic interactions between neurons and astrocytes. The importance of astrocytic functions to neuronal signaling is supported by many experiments reporting high rates of energy consumption and oxidative metabolism in these glial cells. In the brain, almost all energy is consumed by the Na^+/K^+ ATPase, which hydrolyzes 1 ATP to move 3 Na^+ outside and 2 K^+ inside the cells. Astrocytes are commonly thought to be primarily involved in transmitter glutamate cycling, a mechanism that however only accounts for few % of brain energy utilization. In order to examine the participation of astrocytic energy metabolism in brain ion homeostasis, here we attempted to devise a simple stoichiometric relation linking glutamatergic neurotransmission to Na^+ and K^+ ionic currents. To this end, we took into account ion pumps and voltage/ligand-gated channels using the stoichiometry derived from available energy budget for neocortical signaling and incorporated this stoichiometric relation into a computational metabolic model of neuron-astrocyte interactions. We aimed at reproducing the experimental observations about rates of metabolic pathways obtained by ^{13}C-NMR spectroscopy in rodent brain. When simulated data matched experiments as well as biophysical calculations, the stoichiometry for voltage/ligand-gated Na^+ and K^+ fluxes generated by neuronal activity was close to a 1:1 relationship, and specifically 63/58 Na^+/K^+ ions per glutamate released. We found that astrocytes are stimulated by the extracellular K^+ exiting neurons in excess of the 3/2 Na^+/K^+ ratio underlying Na^+/K^+ ATPase-catalyzed reaction. Analysis of correlations between neuronal and astrocytic processes indicated that astrocytic K^+ uptake, but not astrocytic Na^+-coupled glutamate uptake, is instrumental for the establishment of neuron-astrocytic metabolic partnership. Our results emphasize the importance of K^+ in stimulating the activation of astrocytes, which is relevant to the understanding of brain activity and energy metabolism at the cellular level.

Keywords Brain energy metabolism · Potassium · Neuron-astrocyte interactions · Constraint programming · Flux balance analysis

Electronic supplementary material The online version of this article (doi:10.1007/s11064-016-2048-0) contains supplementary material, which is available to authorized users.

✉ Mauro DiNuzzo
mauro.dinuzzo@sund.ku.dk

[1] Center for Basic and Translational Neuroscience, Faculty of Health and Medical Sciences, University of Copenhagen, Blegdamsvej 3B, 24.2.40, 2200 Copenhagen N, Denmark

[2] Museo Storico della Fisica e Centro Studi e Ricerche "Enrico Fermi", Rome, Italy

[3] Fondazione Santa Lucia IRCCS, Rome, Italy

[4] Center for Magnetic Resonance Research, Department of Radiology, Univeristy of Minnesota, Minneapolis, MN, USA

Introduction

One major focus of neuroenergetics research is directed towards the interactions between neuronal and glial cells, the major cellular constituents of the central nervous system. Signaling by neurons and protoplasmic astrocytes indeed controls information processing in the cortical grey matter of the brain. It is now recognized that neurophysiological mechanisms operate under a number of constraints, including cell-specific reaction/transport processes

and their dependence on substrate and energy availability [1, 2]. In particular, these constraints involve delicate balances between substrate supply and demand within specialized cellular metabolic networks counting dozens of coupled biochemical reactions. Although the experimental methods face this complexity with progressively improved technical strategies, computational models remain useful tools in providing interpretative insights to experimental data [3]. In particular, standard as well as probabilistic stoichiometric models have been applied to the study of compartmentalized brain energy metabolism [4–14]. These works have provided valuable insights into specific aspects of neuron-astrocyte interactions, however none have incorporated explicit pathways involved in ion homeostasis (i.e. pumps and channels) related to neurotransmission (see discussion in [6]). In fact, ionic species were present in some stoichiometric models (e.g., [12]) but they were related neither directly nor indirectly with neuronal glutamatergic signaling activity. In the present work we overcame this limitation by taking into account ionic movements across brain cells and the associated energy demand.

The primary aim of the study was to reproduce available experimental findings about the relationship between neuronal activity and cellular energy metabolism, while providing quantitative insights into the neuron-astrocyte functional interactions. We were particularly interested in establishing what triggers the activation of astrocytes during neuronal activity. Indeed, these cells are known to exhibit elevated rates of cerebral oxidative metabolism [15] that cannot be explained by the sole glutamate cycling [16]. In particular, the currently accepted estimates of brain energy utilization for signaling assign to astrocytes only glutamate-related energy use, which represents about 5 % of the total energy budget [1, 17]. However, a number of experimental ^{13}C-MRS studies indicated that astrocytes account for up to 30 % of brain energy metabolism in anesthetized and awake rats (see Table 2 for references). The principal energy-demanding homeostatic function of astrocytes is reuptake of neuronally released K^+ not glutamate (reviewed in [18]), as further evidenced by many studies in cultured astrocytes that have demonstrated that metabolism of these cells is stimulated by K^+ rather than glutamate [19–23]. Besides being energetically expensive, astrocytic K^+ uptake is tightly linked to neuronal activity, because most K^+ is released into extracellular space by neuronal voltage/ligand-gated K^+ channels. Importantly, glutamate reuptake by astrocytes only takes place in perisynaptic astrocytic processes, as glutamate spillover from synaptic cleft is spatially restricted (e.g., [24]). On the contrary, neuronal K^+ release occurs along the length of axons and dendrites and it is thus capable of effectively activating periaxonal and peridendritic peripheral astrocytic processes (>60 % of astrocyte surface area). These notions suggest that the functional and metabolic interactions between neurons and astrocytes might involve primarily K^+ [25].

A recent paper by Leif Hertz and colleagues suggested that astrocytic activation might be induced by the stoichiometry underlying the action of cellular Na^+/K^+ ATPase (NKA), which unevenly transports Na^+ and K^+ across plasma membrane according to a 3/2 ratio [26]. This idea is supported by the facts that (a) during neuronal activity K^+ exits neurons in amounts comparable to the Na^+ entering them [26, 27] and (b) astrocytic but not neuronal NKA is stimulated by excess extracellular K^+ [28–30]. Here we relied on the assumption that neuronal glutamatergic neurotransmission is associated to voltage/ligand-gated ionic currents. This assumption is supported by the finding that, for example, there is proportionality between electroencephalographic signals (related to neuronal activity and therefore to ion movements) and the neurotransmitter cycling rate (which involves glutamate release) in the rat brain over a wide range of conditions (from isoelectric to near-resting levels) [31]. From the perspective of mass-balance modeling, the sole viable approach for implementing such association is to establish a stoichiometric relation between the two processes, keeping in mind that that such stoichiometry in principle might not exist explicitily, but may rather be "hidden" in other mechanisms that are indirectly related to ionic currents. The strategy is similar to what is commonly done for other lumped biochemical reactions (e.g., paracellular diffusion or yield in ATP by the respiratory chain) that are not stoichiometric per se. Therefore, our approach should be considered as a first account on the feasibility of incorporating activity-dependent ionic fluxes in stoichiometric models. Specifically, we tested whether signaling mechanisms in neurons, in terms of glutamate release and aggregated presynaptic and postsynaptic Na^+ and K^+ fluxes, can reproduce experimental observations of activity-induced stimulation of astrocytes in rat brain based on stoichiometry alone.

Methods

We designed a compartmentalized metabolic network made up of blood capillary (b), extracellular space (e) and cellular compartments including neurons (n) and astrocytes (a). In the neuronal and astrocytic elements, we further distinguished cytosol (nc and ac), mitochondria (nm and am) and synaptic vesicles (nv, only in neurons). These cell compartments account for most of tissue volume (e.g., neurons 45–55 %, astrocytes 15–25 %, extracellular space 20 %). We neglected the contribution of GABAergic inhibitory interneurons, as excitatory glutamatergic neurons (85 % of total neurons) and protoplasmic astrocytes are the main cell types within the cortical grey matter of the brain [15]. The network incorporates the main reaction/transport processes of energy

metabolism of carbohydrates in the brain. In addition, we modeled a stoichiometric relation between neuronal glutamate release and voltage/ligand-gated neuronal Na^+ and K^+ currents. Note that neither neuronal nor astrocytic NKA-catalyzed reactions were directly associated to the voltage-gated ion fluxes. As NKA is the principal activity-dependent determinant in ATP hydrolysis, our choice allows investigating the effect of the link between neuronal glutamatergic neurotransmission and associated ion currents on energy metabolism of neurons and astrocytes.

In all simulations, we kept the number of constraints (in addition to the stoichiometry of the metabolic network) to a bare minimum. In particular, we set the upper bound of glutamate-glutamine cycle (Vcyc, defined as $J_{a\rightarrow e}SN$, see Table 1) to $Vcyc^0 = 0.51$ μmol g^{-1} min^{-1}, which is the value obtained with ^{13}C nuclear magnetic resonance spectroscopy (MRS) in awake rats [32]. Such a procedure is equivalent to introduce an arbitrary numeric scaling factor for the output fluxes, which in itself cannot be considered as a constraint. The sole hard constraint we introduced was the fraction of energy used by signaling versus that used by housekeeping functions. Specifically, we constrained the sum of neuronal plus astrocytic ATPase fluxes directed to housekeeping in the range 3–6 μmol g^{-1} min^{-1}, or ~10–20% of glucose utilization [33], assuming 32 ATP molecules produced per glucose metabolized and a cerebral metabolic rate of glucose of 0.91 μmol g^{-1} min^{-1} [32]. It is noted that at the whole-brain level (i.e. including white-matter), the fraction of energy allocated to housekeeping is somewhat greater, with different estimates giving values ranging from 25% in rodents [16, 34] to 50% in humans [35] (with the latter value likely overestimated, see [33] and references therein). Altogether, the metabolic network consists of 120 metabolites and 119 fluxes (Table 1). A brief description of the pathways included in the present model is provided in Online Resource 1. We also provide the model containing all reaction/transport fluxes in the System Biology Markup Language (SBML) format (Online Resource 2).

The sampling algorithm used to obtain distribution of fluxes was developed employing constraint logic programming (CLP) over real numbers (CLPR) [36]. The details of the CLP-based sampling algorithm implemented to solve flux balance analysis (FBA) problems, as well as convergence diagnostics and benchmarking against the Artificial Centering Hit-and-Run algorithm, are given in Online Resource 3. Briefly, given a set of variables (fluxes) and constraints (stoichiometry), the algorithm iteratively binds a variable (randomly from the set of variables) to a value (randomly from the variable domain). This binding represent a further constraint, which eventually reduces the domains of the other unbound variables [37]. If these additional constraints result in inconsistent domain for some unbound variables, then the algorithm restarts with all unbounds variables, otherwise the solution is valid and it is recorded. The algorithm was implemented under SWI Prolog (University of Amsterdam, The Netherlands; http://www.swi-prolog.org) running the built-in CLPR library. Results of the simulations were analyzed using MATLAB (The Mathworks Inc., Natick, MA, USA; http://www.mathworks.com/).

Results

We first determined the initial domains of the fluxes underlying our metabolic network (see Online Resource 4). The pruning of solution space brought about by CLP is remarkable, with most fluxes constrained to values below 5 μmol g^{-1} min^{-1} and maximal range of about 12 μmol g^{-1} min^{-1}. It should be noted that the actual solutions (i.e. the distributions obtained through sampling) will map a subset of the variable domains depending on the specified constraints.

The stoichiometry of the metabolic network is almost completely determined by biochemical reaction/transport processes. However, the quantitative mass-balance underlying the relation between glutamate release and ionic movements is unknown. Based on biophysical calculations it has been estimated that about 400,000 Na^+ ions enter neurons through voltage/ligand-gated channels (i.e. aggregated for presynaptic and postsynaptic currents) per each glutamate vesicle released [16]. Assuming an average vesicular content in the range of 2000–6000 glutamate molecules [38–41] gives a flux of 60–200 Na^+ ions per glutamate molecule. We found that a value around the low-end of 60 Na^+ per glutamate (for sodium influx and also for potassium efflux, see below) correctly reproduces the experimental relationship between the rates of glutamate-glutamine cycle and neuronal oxidative metabolism (Fig. 1a). The Na^+ influx and K^+ efflux underlying neuronal signaling are thought to be of comparable magnitude. However, the (electrogenic) NKA responsible of restoring ion concentrations operates with a 3/2 Na^+/K^+ flux ratio. The resulting imbalance between Na^+ and K^+ ionic movements (inward Na^+/outward K^+ due to neuronal activity and outward Na^+/inward K^+ due to NKA) produces an excess K^+ in the extracellular space, which is likely removed by astrocytes [26]. Our model fully supports this notion. Simulations performed with various neuronal voltage/ligand-gated Na^+/K^+ influx/efflux ratios largely determined the degree of astrocytic activation, which is completely abolished when the ratio is close to 3/2 (Fig. 1b). Overall, using a 63/58 Na^+/K^+ ratio for neuronal ionic fluxes (Fig. 2), the cellular rates of metabolic pathways for oxidative metabolism of glucose are consistent with experimental data (Fig. 1; Table 2).

We found that the experimentally observed rate of pyruvate carboxylation at $Vcyc = Vcyc^0 = 0.51$ μmol g^{-1} min^{-1}

Table 1 Stoichiometry of reaction/transport fluxes constituting the metabolic network

Flux name	Stoichiometry	Enzyme/transporter/process
Glutamatergic activity (including neurotransmission, ionic movements and glutamate-glutamine cycle)		
J_nNT	$GLU_{nv} + a\ Na_e + b\ K_n \rightarrow GLU_e + a\ Na_n + b\ K_e$	Glutamatergic neurotransmission GLU: glutamate Na: sodium K: potassium
$J_{e\rightarrow a}$EAAT	$GLU_e + 3\ Na_e + K_a \rightarrow GLU_{ac} + 3\ Na_a + K_e$	Excitatory amino acid transporter (EAAT)
J_nVGLUT	$GLU_{nc} + 1.5\ ATP_n \rightarrow GLU_{nv} + 1.5\ ADP_n$	Vesicular glutamate transporter (VGLUT) ATP: adenosine triphosphate ADP: adenosine diphosphate
J_xNKA	$3\ Na_x + 2\ K_e + ATP_x \rightarrow 3\ Na_e + 2\ K_x + ADP_x$	Neuronal/astrocytic Na/K-activated ATPase (NKA)
$J_{a\rightarrow n}$KIR	$K_a \rightarrow K_n$	K inward rectifying (KIR) channels
J_aNax	$Na_e \rightarrow Na_a$	Astrocytic Na-sensing Na channel (Nax)
J_aGS	$GLU_{ac} + ATP_a + NH_{4,a} \rightarrow GLN_a + ADP_a$	Astrocytic glutamine synthetase (GS) NH_4: ammonia GLN: glutamine
$J_{a\rightarrow e}$SN (V_{cyc})	$GLN_a \rightarrow GLN_e$	Astrocytic glutamine system N (SN) transporter
$J_{e\rightarrow n}$SA	$GLN_e + Na_e \rightarrow GLN_n + Na_n$	Neuronal glutamine system A (SA) transporter
J_nPAG	$GLN_n \rightarrow GLU_{nc} + NH_{4,n}$	Neuronal phosphate-activated glutaminase (PAG)
Blood–brain nutrients (glucose/oxygen) transport		
$J_{b\rightarrow e}$GLUT	$GLC_b \rightarrow GLC_e$	Blood–brain glucose transporter (GLUT) GLC: glucose
$J_{e\rightarrow x}$GLUT	$GLC_e \rightarrow GLC_x$	Neuronal/astrocytic glucose transporter (GLUT)
$J_{\rightarrow b}O_2$	$\rightarrow O_{2,b}$	Blood oxygen diffusion (entry) O_2: oxygen
$J_{b\rightarrow x}O_2$	$O_{2,b} \rightarrow O_{2,x}$	Oxygen diffusion to neuron/astrocyte
$J_{x\rightarrow b}CO_2$	$CO_{2,x} \rightarrow CO_{2,b}$	Carbon dioxide diffusion to blood CO_2: carbon dioxide
$J_{b\rightarrow}CO_2$	$CO_{2,b} \rightarrow$	Blood carbon dioxide diffusion (exit)
Intercellular lactate trafficking		
$J_{x\leftrightarrow e}$MCT	$LAC_x \leftrightarrow LAC_e$	Neuronal/astrocytic monocarboxylate transporter (MCT) LAC: lactate
Glycolysis (Embden–Meyerhof–Parnas pathway)		
J_xHK	$GLC_x + ATP_x \rightarrow G6P_x + ADP_x$	Neuronal/astrocytic hexokinase (HK) G6P: glucose 6-phosphate
J_xPGI	$G6P_x \leftrightarrow F6P_x$	Neuronal/astrocytic phosphoglucoisomerase (PGI) F6P: fructose 6-phosphate
J_xPFK	$F6P_x + ATP_x \rightarrow FBP_x + ADP_x$	Neuronal/astrocytic phosphofructokinase (PFK) FBP: fructose 1,6-bisphosphate
J_xALD	$FBP_x \leftrightarrow GAP_x + DHAP_x$	Neuronal/astrocytic aldolase (ALD) GAP: glyceraldehyde 3-phosphate DHAP: dihydroxyacetone phosphate
J_xTPI	$DHAP_x \leftrightarrow GAP_x$	Neuronal/astrocytic triosephosphate isomerase (TPI)
J_xGAPDH	$GAP_x + NAD_x \leftrightarrow BPG_x + NADH_x$	Neuronal/astrocytic glyceraldehyde 3-phosphate dehydrogenase (GAPDH) NAD(H): nicotinamide adenine dinucleotide BPG: 1,3-bisphosphoglycerate
J_xPGK	$BPG_x + ADP_x \leftrightarrow 3PG_x + ATP_x$	Neuronal/astrocytic phosphoglycerate kinase (PGK) 3PG: 3-phosphoglycerate
J_xPGM	$3PG_x \leftrightarrow 2PG_x$	Neuronal/astrocytic phosphoglycerate mutase (PGM) 2PG: 2-phosphoglycerate
J_xENO	$2PG_x \leftrightarrow PEP_x$	Neuronal/astrocytic enolase (ENO) PEP: phosphoenolpyruvate

Table 1 (continued)

Flux name	Stoichiometry	Enzyme/transporter/process
J_xPK	$PEP_x + ADP_x \rightarrow PYR_x + ATP_x$	Neuronal/astrocytic pyruvate kinase (PK) PYR: pyruvate
J_xLDH	$PYR_x + NADH_x \leftrightarrow LAC_x + NAD_x$	Neuronal/astrocytic lactate dehydrogenase (LDH) LAC: lactate
Pyruvate recycling		
J_x(c/m)ME	$MAL_{x(c/m)} + NADP_{x(c/m)} \rightarrow PYR_{x(c/m)} + NADPH_{x(c/m)}$	Neuronal/astrocytic cytosolic/mitochondrial malic enzyme (ME) MAL: malate NADP(H): nicotinamide adenine dinucleotide phosphate
Pyruvate carboxylation (anaplerosis)		
J_aPC	$PYR_{am} + ATP_a \rightarrow OAA_{am} + ADP_a$	Astrocytic pyruvate carboxylase (PC) OAA: oxaloacetate
Tricarboxylic acid (TCA) cycle (Krebs cycle)		
J_xmMCT	$PYR_{xc} \leftrightarrow PYR_{xm}$	Neuronal/astrocytic mitochondrial monocarboxylate transporter (mMCT)
J_xPDH	$PYR_{xm} + CoA_x + NAD_{xm} \rightarrow ACoA_x + CO_{2,x} + NADH_x$	Neuronal/astrocytic pyruvate dehydrogenase (PDH) CoA: coenzyme A ACoA: acetyl-coenzyme A
J_xCS	$OAA_{xm} + ACoA_x \rightarrow CIT_x + CoA_x$	Neuronal/astrocytic citrate synthase (CS) CIT: citrate
J_xACO	$CIT_x \leftrightarrow ISO_{xm}$	Neuronal/astrocytic mitochondrial aconitase (ACO) ISO: isocitrate
J_xIDH1/2/3	(1) $ISO_{xm} + NAD_{xm} \rightarrow AKG_{xm} + CO_{2,x} + NADH_{xm}$ (2) $ISO_{xm} + NADP_{xm} \rightarrow AKG_{xm} + CO_{2,x} + NADPH_{xm}$ (3) $ISO_{xc} + NADP_{xc} \rightarrow AKG_{xc} + CO_{2,x} + NADPH_{xc}$	Neuronal/astrocytic cytosolic/mitochondrial isocitrate dehydrogenase (IDH) AKG: α-ketoglutarate (oxoglutarate)
J_xAKGDH	$AKG_{xm} + CoA_x + NAD_{xm} \rightarrow SCoA_x + CO_{2,x} + NADH_{xm}$	Neuronal/astrocytic α-ketoglutarate dehydrogenase (AKGDH) SCoA: succinyl coenzyme A
J_xSCS	$SCoA_x + ADP_x \leftrightarrow SUC_x + CoA_x + ATP_x$	Neuronal/astrocytic succinyl coenzyme A synthetase (SCS) SUC: succinate
J_xSDH	$SUC_x + (2/3)\ NAD_{xm} \leftrightarrow FUM_x + (2/3)\ NADH_{xm}$	Neuronal/astrocytic succinate dehydrogenase (SDH) FUM: fumarate
J_xFUM	$FUM_x \leftrightarrow MAL_{xm}$	Neuronal/astrocytic fumarase (FUM)
J_x(c/m)MDH	$OAA_{x(c/m)} + NADH_{x(c/m)} \rightarrow MAL_{x(c/m)} + NAD_{x(c/m)}$	Neuronal/astrocytic cytosolic/mitochondrial malate dehydrogenase (MDH)
Mitochondrial carriers		
J_xGC	$GLU_{xc} \leftrightarrow GLU_{xm}$	Neuronal/astrocytic mitochondrial glutamate carrier (GC)
J_xDCC	$MAL_{xm} \leftrightarrow MAL_{xc}$	Neuronal/astrocytic mitochondrial dicarboxylate carrier (DIC)
J_xCIC	(1) $ISO_{xm} \leftrightarrow ISO_{xc}$ (2) $CIT_{xm} \leftrightarrow CIT_{xc}$	Neuronal/astrocytic mitochondrial citrate-isocitrate carrier (CIC)
Fatty acid synthesis (shunt)		
J_xACL	$CIT_{xc} + ATP_x + CoA_x \rightarrow OAA_{xc} + ADP_x + ACoA_x$	Neuronal/astrocytic ATP citrate lyase (ACL)
Mitochondrial NADH shuttles		
J_xG3PS	$NADH_{xc} + (2/3)\ NAD_{xm} \rightarrow NAD_{xc} + (2/3)\ NADH_{xm}$	Neuronal/astrocytic glycerol 3-phosphate shuttle (G3PS)
J_xOGC	$MAL_{xc} + AKG_{xm} \rightarrow MAL_{xm} + AKG_{xc}$	Neuronal/astrocytic oxoglutarate carrier (OGC)
J_xAGC	$GLU_{xc} + ASP_{xm} \rightarrow GLU_{xm} + ASP_{xc}$	Neuronal/astrocytic aspartate-glutamate carrier (AGC) ASP: aspartate
J_x(c/m)AAT	$ASP_{x(c/m)} + AKG_{x(c/m)} \leftrightarrow OAA_{x(c/m)} + GLU_{x(c/m)}$	Neuronal/astrocytic cytosolic/mitochondrial aspartate aminotransferase (AAT)

Table 1 (continued)

Flux name	Stoichiometry	Enzyme/transporter/process
Ammonia homeostasis		
J_xGDH	$GLU_{xm} + NAD_{xm} \leftrightarrow AKG_{xm} + NADH_{xm} + NH_{4,x}$	Neuronal/astrocytic glutamate dehydrogenase (GDH)
J_xALAT	$GLU_{xm} + PYR_{xm} \leftrightarrow AKG_{xm} + ALA_x$	Neuronal/astrocytic alanine aminotransferase (ALAT) ALA: alanine
$J_{x\leftrightarrow e}$ALA	$ALA_x \leftrightarrow ALA_e$	Neuronal/astrocytic alanine transporter
J_xBCAT	$GLU_{xm} + BCKA_x \leftrightarrow AKG_{xm} + BCAA_x$	Neuronal/astrocytic branched-chain aminotransferase (cBCAT) BCKA: branched-chain keto acid BCAA: branched-chain amino acid
$J_{x\leftrightarrow e}$BCAA	$BCAA_x \leftrightarrow BCAA_e$	Neuronal/astrocytic branched-chain amino acid transporter
$J_{x\leftrightarrow e}$BCKA	$BCKA_x \leftrightarrow BCKA_e$	Neuronal/astrocytic branched-chain keto acid transporter
Oxidative phosphorylation		
J_xOP	$2\ NADH_{xm} + 5\ ADP_x + O_{2,x} \rightarrow 2\ NAD_{xm} + 5\ ATP_x + c\ ROS_x$	Neuronal/astrocytic respiration ROS: reactive oxygen species
Housekeeping		
J_xATPase	$ATP_x \rightarrow ADP_x$	Neuronal/astrocytic ATPases (other than NKA)
Antioxidant system		
J_xPPP	$3\ G6P_x + 6\ NADP_{xc} \rightarrow GAP_x + 2\ F6P_x + 6\ NADPH_{xc}$	Neuronal/astrocytic pentose phosphates pathway
J_x(c/m)GR	$GSSG_x + NADPH_{x(c/m)} \rightarrow 2\ GSH_x + NADP_{x(c/m)}$	Neuronal/astrocytic cytosolic/mitochondrial glutathione reductase (GR) GSSG: glutathione disulfide GSH: glutathione
J_xGPX	$2\ GSH_x + ROS_x \rightarrow GSSG_x$	Neuronal/astrocytic glutathione peroxidase

Subscripts indicate tissue compartments (see text). Subscript x indicates either n (neuronal) or a (astrocytic) compartment

In the stoichiometry equations the single and double arrows represent irreversible and reversible fluxes, respectively

Optimized stoichiometric coefficients for NKA-catalyzed reactions are a = 63 and b = 58. Optimized stoichiometric coefficient for ROS generation in oxidative phosphorylation are c = 0.025 (neurons) and c = 0.250 (astrocytes)

(awake value) is obtained by assuming that astrocytic production of ROS per oxygen consumed is tenfold higher than neurons (Fig. 1c), which possibly reflects a lower activity/expression of mitochondrial bound kinases, as previously suggested [18]. As expected, ROS generation affects the rate of PPP, which turns out to be several-fold higher in astrocytes compared with neurons (8–11 nmol g^{-1} min^{-1} vs. 2 nmol g^{-1} min^{-1}, see Online Resource 10 Panels N,T), which is consistent with current literature ([55] and references therein). The activity-dependent increase in PC rate due to ROS scavenging is brought about by the regeneration of NADPH through pyruvate-malate shuttle. This pathway makes PC activity independent of any carbon loss from the astrocytic TCA cycle (see below). It is noted that other mechanisms might participate in stimulating astrocytic PC rate, such as glutamine and/or citrate efflux (see Online Resource 1), that could be fine-tuned to obtain similar model outcomes.

Model results are consistent with the experimentally measured rates of both cerebral glucose (Fig. 3a) and oxygen (Fig. 3b) utilization and associated range of oxygen-to-glucose index (OGI) (Fig. 3c). Simulated values for cell oxidative metabolism are in very good agreeement with experimental ^{13}C-MRS data. In particular, the simulated reaction rates of neuronal (Fig. 3d) and astrocytic (Fig. 3e) pyruvate dehydrogenase as well as the rate of astrocytic pyruvate carboxylase (Fig. 3f) at $Vcyc = Vcyc^0$ match on average the experimental values of 1.16, 0.30 and 0.18 μmol g^{-1} min^{-1} measured under awake conditions in rat brain [32], respectively.

Under the conditions that reproduced the aforementioned experimental results, simulations showed that glucose is on average almost equally taken up by neurons and astrocytes (Fig. 4a, b) while intercellular lactate trafficking is negligible (Fig. 4d, e). In fact, there are slightly more solutions supporting a predominant neuronal glucose uptake and associated lactate release (Fig. 4c). The preference for a small lactate transfer (0.05 μmol g^{-1} min^{-1}) from neurons to astrocytes under awake conditions supports recent modeling studies [56, 57]. However, there is no apparent correlation between intercellular lactate trafficking and neurotransmission level, in agreement with our previous theoretical analysis [6]. In fact, it is the exact value of glucose partitioning between the two cell types to completely determine the direction and magnitude of lactate transfer (Fig. 4f), as previously reported [5, 6]. On average, simulations show

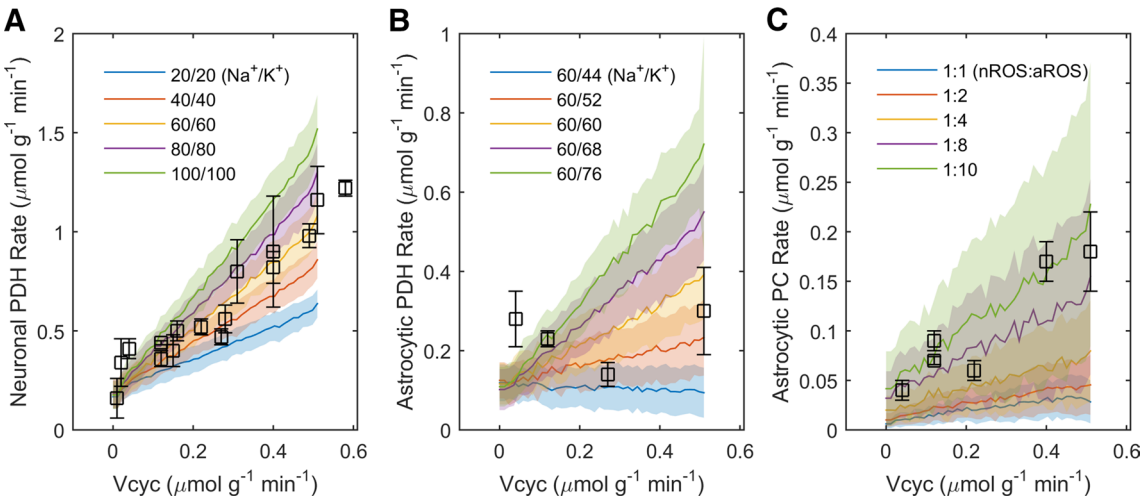

Fig. 1 Validation of the model against experimental data. The agreement between simulations and specific experimentally measured fluxes has been examined at the stoichiometric level (i.e. without introducing constraints in addition to the metabolic network). **a** Neuronal PDH rate is controlled by the absolute amount of Na^+ (K^+) ions entering (exiting) the cell per transmitter released, here always in a 1:1 ratio. The optmized value is 63 ions moving per each glutamate molecule. **b** Astrocytic PDH rate is controlled by the imbalance between neuronal voltage/ligand-gated Na^+ and K^+ ionic currents. The optimized proportion is 58 K^+ exiting neurons during concomitant entry of 63 Na^+ per each glutamate molecule. Note that neuronal and astrocytic PDH rates depends on the energy expended by NKA to move Na^+ and K^+ in opposite direction relative to depolarization/hyperpolarization underlying neuronal activity. While neuronal metabolism is sensitive to the magnitude of Na^+ influx/K^+ efflux, astrocytic metabolism responds to the imbalance between those fluxes. **c** Astrocytic PC rate is controlled by the relative rate of ROS production in astrocytes compared with neurons. The optimized value is a tenfold higher ROS production in astrocytes relative to neurons. Simulated values are expressed as mean ± SD. Experimental data points are listed in Table 2

that under awake conditions neurons and astrocytes take up a similar fraction of glucose (~0.35 μmol g^{-1} min^{-1}, respectively).

In order to examine how the participation of astrocytes in neuronal activity affects the metabolic network of both cell types, we performed correlation analysis of fluxes (Fig. 5). The spread matrix shows that cellular glycolysis is strongly correlated within each individual cell types and strongly anticorrelated with the other cell type. Interestingly, the opposite is true, although less firmly, for cellular TCA cycle. In other words, there is a positive correlation between neuronal glycolysis and astrocytic TCA cycle, and vice versa. Interestingly, this behavior depends on the amount of neuronally released K^+ (due to voltage/ligand-gated channels) in excess of the 3/2 Na^+/K^+ NKA ratio (Fig. 6). These results (and in particular, the loss of intercellular correlation) are obtained even in the presence of glutamatergic neurotransmission and glutamate-glutamine cycle, supporting the idea that astrocytic K^+ uptake is the major mechanism underlying the metabolic relationship between neurons and astrocyte. This finding is further strengthened by the fact that blocking extracellular glutamate reuptake by astrocytes (and concomitantly allowing glutamate uptake directly by neurons) does not alter the correlation patterns between glycolysis and TCA cycle (Online Resource 5).

Finally, we compared flux distributions and corresponding average values obtained for the whole range of neuronal activity levels ($0 \le Vcyc \le Vcyc^0$; $Vcyc^0 = 0.51$ μmol g^{-1} min^{-1}) with those obtained for the sole awake conditions ($Vcyc = Vcyc^0$) (Online Resources 6–10 and 11–15, respectively). As expected, the distributions of fluxes change under awake conditions, confirming that fluxes are modulated by neuronal activity. However, there are certain fluxes exhibiting nearly the same distribution regardless of the activation state. These activity-independent fluxes include MCT (Online Resource 6 Panels U,V; compare with Online Resource 11 Panels U,V) and LDH (Online Resource 7 Panels I,V; compare with Online Resource 12 Panels I,V). This result indicates that cell-specific lactate production/utilization and cell-to-cell lactate shuttling are not constrained in any direction by the activity levels, as further support to previous modeling study [6]. As expected, the metabolic fluxes whose domains collapse into a single value (0.51 μmol g^{-1} min^{-1}) when $Vcyc = Vcyc^0$ are those involved in glutamate-glutamine cycle (Online Resource 6 Panels H,K; compare with Online Resource 11 Panels H,K) and associated ammonia homeostasis (Online Resources 9 Panel A and Online Resource 10 Panel F; compare with Online Resource 14 Panel A and Online Resource 15 Panel F). The distribution of fluxes for the whole metabolic network are provided as evidence for the good performance of our sampling algorithm. The archives containing the complete datasets for unconstrained and awake conditions are provided in Online Resource 16.

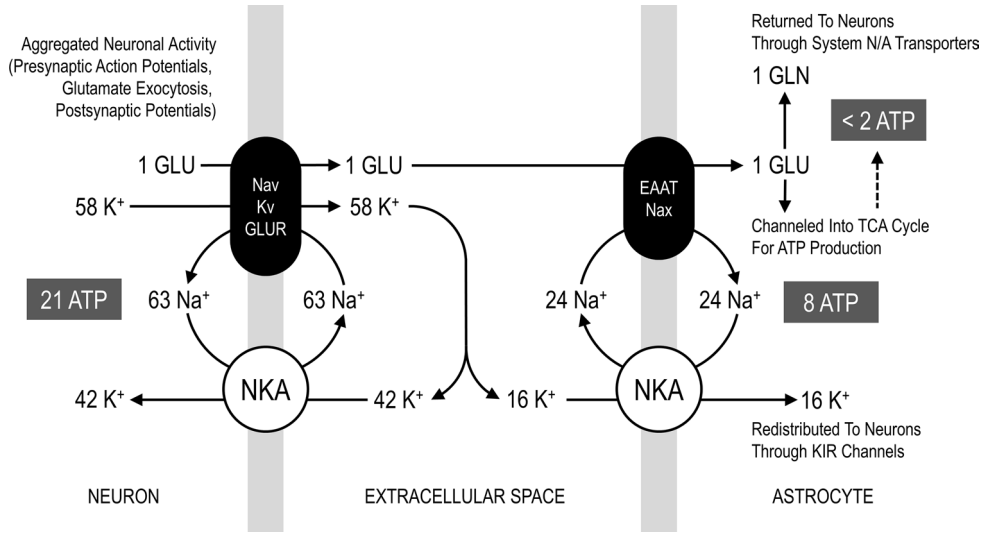

Fig. 2 Stoichiometry for voltage/ligand-gated Na^+ and K^+ channel currents associated with neuronal glutamatergic neurotransmission. Simplified schematics of the stoichiometric relation between the exocytosis of 1 glutamate molecule, influx of 63 Na^+ ions (i.e. depolarization) and efflux of 58 K^+ ions (i.e. repolarization). These values are the results of the fitting procedure between model outcomes and experimental ^{13}C-MRS obtained in rat brain during different activity levels (see Fig. 1). The corresponding ratio between Na^+ and K^+ fluxes due to neuronal activity is thus close to 1:1. Yet, NKA (both neuronal and astrocytic) works in a 3/2 Na^+/K^+ ratio. Therefore, only part of neuronally released K^+ (42/58, i.e. around 72 %) is taken up directly by these cells, with concomitant hydrolysis of 21 ATP molecules. The difference in the magnitude of ionic currents underlying neuronal activity and the opposite ionic movements underlying NKA action in neurons results in an excess of 16 K^+ ions in extracellular space, which are actively taken up by astrocytes and passively redistributed to neurons. Overall, the astrocytic uptake of the fraction of neuronally released K^+ (16/58, i.e. around 28 %) is associated with the hydrolysis of 8 ATP molecules. At the same time, the glutamate molecule is taken up and converted to glutamine, with an associated hydrolysis of 1–2 ATP molecules (notice that glutamate reuptake is also associated with corelease of 1 K^+, not shown in the figure). However, the latter number is also reduced by the fact that some glutamate is channeled into TCA cycle, thereby providing ATP for its own uptake. The above-mentioned processes provide the following energy budget for signaling (i.e. excluding housekeeping): nearly 67.5 % of energy is used by neuronal glutamatergic activity, 26 % by astrocytic K^+ reuptake and 6.5 % for glutamate recycling. Astrocytic energy expenditure accounts for one-third of the total, most of which (~80 %) is devoted to active K^+ reuptake. Please note that Na^+ cycle in astrocytes can be supported by many pathways other than the extracellular Na^+-sensitive Na^+ channel (Nax) and excitatory amino acid transporter (EAAT) proteins (see Online Resource 1)

Discussion

In the last years, novel thoughts have stimulated revisions of long-established notions about the metabolic pathways used to sustain brain function. An intense area of research has focused on the participation of astrocytes in virtually any aspects of neuronal signaling. In the cortical gray matter of the brain, these cells constitute nearly 20 % of brain tissue volume and account for up to 30 % of oxidative metabolism [15]. These relatively high metabolic rates, which per volume are comparable to those of neurons, could not be reproduced by theoretical studies that based astrocytic energy demand exclusively on recycling of transmitter glutamate (e.g., [16]). As we illustrated in the introduction, this latter assumption has contributed to promote the wrong notion that cortical astrocytes consume only few % of the brain's energy budget. In recent years, it has become more and more clear that astrocytes are far more sensitive to increases in extracellular K^+ than glutamate (reviewed by [18]). This means that any quantitative model of neuron-astrocyte interactions must take into account the contribution of astrocytes in the energy-requiring process of K^+ uptake. Due to the difficulty of determing this contribution quantitatively, many mathematical models neglected tout-court astrocytic involvement in ion homeostasis and correspondingly underestimated activation of astrocytes and associated energy consumption. Here, we took advantage of experimental results obtained with ^{13}C-MRS in rat brain, and determined a simple stoichiometric relation between glutamatergic neurotransmission and voltage/ligand-gated Na^+ and K^+ ion fluxes in neurons. We found that the 63/58 Na^+ influx/K^+ efflux per glutamate molecule underlying neuronal activity (see Fig. 1) is sufficient to reproduce the experimental measurements of major neuronal and, notably, astrocytic metabolic pathways (Figs. 2, 3, 4). In particular, the imbalance between the above-mentioned activity-dependent ion movements ratio (close to 1:1) and the 3/2 outward Na^+/inward K^+ NKA ratio can itself explain the finding that astrocytes account for nearly one-third of total brain energy metabolism.

Our results indicate that the experimental relationship between glutamate-glutamine cycle (Vcyc) and cellular

oxidative metabolism of glucose (i.e. PDH reaction rate) is dictated for neurons by the absolute amount of neuronal Na^+ and K^+ ionic fluxes (Fig. 2a), and for astrocytes by the imbalance between these fluxes (Fig. 2b). The rate of astrocytic PC is instead not directly related to ionic movements. The choice to avoid assumptions on the loss of TCA cycle intermediates resulted in the finding that PC is only indirectly correlated to neuronal activity through the activity-dependent increase in ROS scavenging (Fig. 2c). The biochemical mechanism for increased PC rate and antioxidant system is the replenishment of the NADPH required by glutathione reductase. Specifically, combined action of malic enzyme and PC regenerates NADPH with concomitant hydrolysis of ATP. These reactions (pyruvate-malate shuttle) bypass the NADH-yielding malate dehydrogenase step of TCA cycle, which converts malate to oxaloacetate. Notably, PC activity becomes negatively correlated with PPP in astrocytes (Fig. 5), the other NADPH-producing pathway. However, the negative correlation between PC and PPP does not necessarily mean that PC is the primary mechanism for detoxification of ROS. Indeed, the model supports the notion that NAPDH is regenerated through PPP in an activity-dependent manner, as evidenced by the positive correlation between PPP and neuronal ionic currents and neurotransmission (Fig. 5). In other words, while PC and PPP are negatively correlated to each other, both are positively correlated with glutamatergic activity. The above-mentioned scenario depends on our choice to avoid assumptions about any activity-dependent loss of astrocytic TCA cycle intermediates (see Online Resource 1), as the exact biochemical mechanisms underlying the change in PC rate associated with activity levels remain to be experimentally established.

Overall, it is the departure of neuronal voltage/ligand-gated Na^+ and K^+ fluxes from the Na^+/K^+ NKA-dependent fluxes (1:1 for the former and 3/2 for the latter) that is primarily responsible for the establishment of the link between neuronal and astrocytic metabolism (Fig. 6). In particular, at increasing rates of K^+ release relative to Na^+, the neuronal glucose utilization (determined by HK reaction rate) becomes more and more correlated with astrocytic oxidative metabolism (determined by PDH reaction rate). This finding is consitent with the rise in astrocytic respiration induced by K^+ reported experimentally (see [15]). We found that glutamate, which is commonly thought to represent the primary signal linking neuronal and astrocytic functional metabolism, does not appreciably affect the correlation patterns between cellular metabolic pathways (Online Resource 5). We also found that K^+ uptake in astrocytes is necessary for the activity-dependent upregulation of energy metabolism in these cells, which is evidenced by the finding that under certain conditions astrocytic metabolism remains low even when glutamate-glutamine cycle increases (e.g., see Fig. 1b). Indeed, glutamate uptake by astrocytes requires much less energy than K^+. According to our estimates, nearly 16 K^+ ions (Fig. 2) enter astrocytes per each glutamate, thus requiring 8 ATP molecules (as NKA takes up 2 K^+ per ATP hydrolyzed). Since the cycling of one glutamate molecule by astrocytes requires hydrolysis of two ATP molecules (reuptake plus conversion to glutamine), this means that overall energy consumption in astrocytes due to K^+ uptake is about fourfold higher than that required by uptake of glutamate. Furthermore, glutamate but not K^+ can be used as energy substrate to fuel its own uptake, which can even lower the energetic burden of astrocytes for glutamate uptake [58, 59].

The model upholds the concept that neurons and astrocytes can use whatever proportion of glucose and lactate (Fig. 4). Depending on cellular glucose uptake, lactate

Table 2 Metabolic fluxes measured with ^{13}C-MRS in adult rat gray matter under different activity levels

References	Vcyc	J_nPDH	J_aPDH	J_aPC
Deep anesthesia (isoelectric EEG)				
[42]	0.01 ± 0.01	0.16 ± 0.10	–	–
[43]	0.02 ± 0.01	0.34 ± 0.12	–	–
[44]	0.04 ± 0.01	0.41 ± 0.05	0.28 ± 0.07	0.04 ± 0.01
Moderate anesthesia				
[42]	0.15 ± 0.05	0.40 ± 0.08	–	–
[45]	0.12 ± 0.01	0.44 ± 0.01	0.23 ± 0.02	0.070 ± 0.004
[46, 47]	0.22 ± 0.04	0.52 ± 0.04	–	0.06 ± 0.01[a]
[48]	0.12 ± 0.01[c]	0.36 ± 0.04[c]	–	0.09 ± 0.01[d]
[49]	0.27 ± 0.02	0.47 ± 0.04	0.14 ± 0.03	–
[50]	0.16 ± 0.04	0.50 ± 0.05	–	–
Light anesthesia				
[51]	0.28 ± 0.03	0.56 ± 0.07	–	–
[48]	0.40 ± 0.04[c]	0.82 ± 0.08[c]	–	0.17 ± 0.02[d]
[42]	0.40 ± 0.13	0.90 ± 0.28	–	–
[52]	0.31 ± 0.17	0.80 ± 0.16	–	–
[43]	0.58 ± 0.02	1.22 ± 0.04	–	–
Awake				
[53]	0.49 ± 0.05[b]	0.98 ± 0.06[b]	–	–
[32]	0.51 ± 0.21	1.16 ± 0.17	0.30 ± 0.11	0.18 ± 0.04

All values are expressed in units μmol g^{-1} min^{-1} (mean ± SD). Approximate state of the animals range from deep, moderate, light anesthesia to awake, as indicated. These conditions are associated with the different metabolic rates plotted in Fig. 1. For details about experimental conditions (e.g., employed anesthetics) see individual studies. Some data appear as they were reanalyzed elsewhere [33, 54]

[a]Estimated based on identical values of neuronal PDH in two different studies under the same experimental conditions

[b]Averaged from frontal, parietal, temporal and occipital cortex

[c]Error estimated as 10% of the experimental measurement, which corresponds to the average error of tabulated studies

[d]Calculated from measured ratio between PC and neuronal PDH

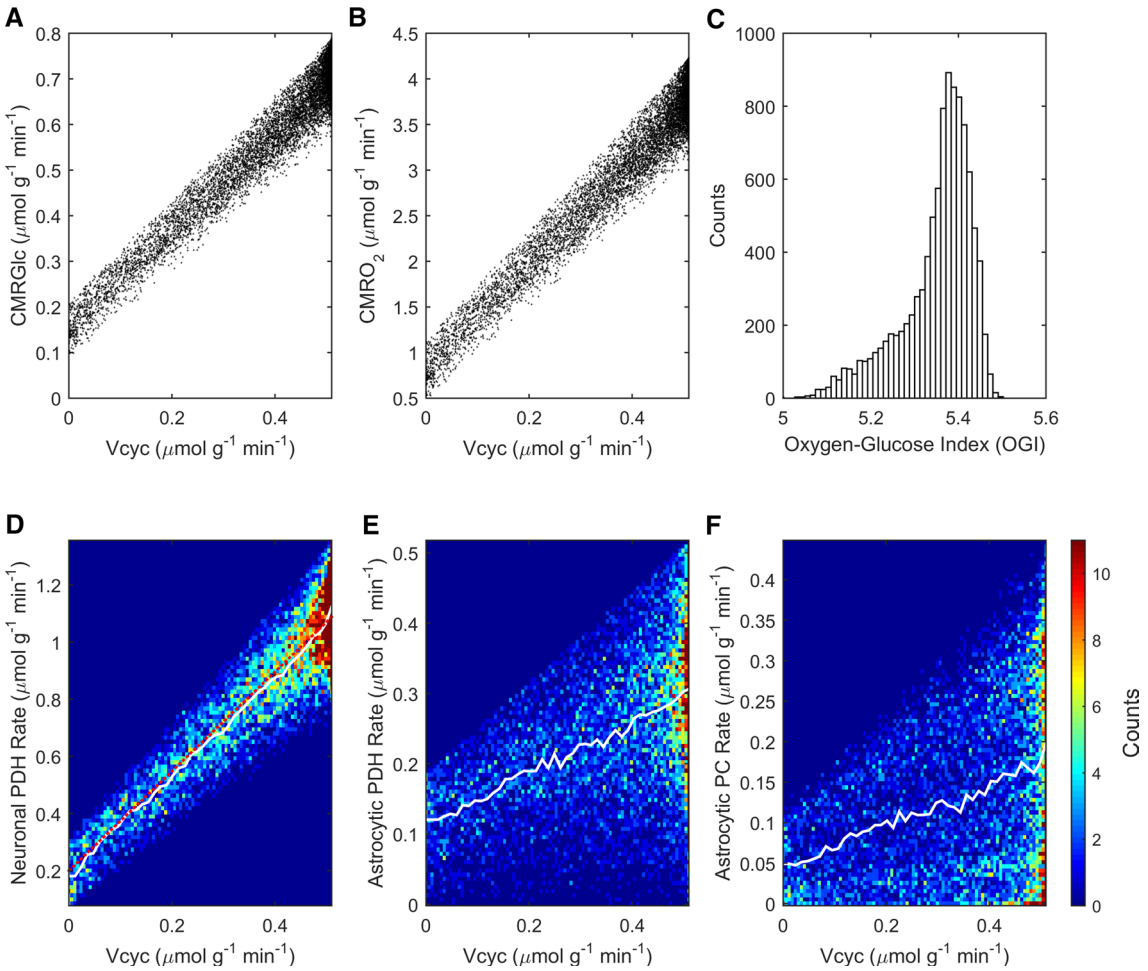

Fig. 3 Model outcomes for tissue and cellular oxidative metabolism. The simulated fluxes of cerebral metabolic rate of **a** glucose (CMRGlc) and **b** oxygen ($CMRO_2$) are associated with a range of **c** oxygen-to-glucose index (OGI) that is consistent with the reported values measured experimentally. **d–f** Results of optimization of stoichiometric coefficients (see Table 1; Fig. 1) for neuronal PDH, astrocytic PDH and astrocytic PC, respectively. Counts in different panels refer to the actual number of solutions falling in a given bin (either color-coded or as histogram), which sum up to 10,000. *Color plots* have been obtained by computing the histograms of solutions (bins number determined according to Rice rule, or $2n^{1/3}$, where n is the total number of solutions). Note that the upper bound of the abscissa in panels **a, b, d, e, f** is at $Vcyc = Vcyc^0 = 0.51$ μmol g^{-1} $min^{-}1$ (awake value). (Color figure online)

transport across cells is indeed adjusted to satisfy neuronal and astrocytic energy needs, as previously reported [3]. In particular, the stoichiometry is compatible with model solutions identifying one cell type as the sole compartment of glucose uptake and lactate release and the other cell type relying completely on lactate uptake. Since we decided to avoid the introduction of additional constraints to restrict the space of feasible solutions, we interpret such extreme cases as reflecting a lack of information in the present model (e.g. incomplete metabolic network and/or absence of regulatory mechanisms). In fact, these cases with poor physiological significance are canceled out by averaging across solutions. The distributions-based approach provides complementary information to objective-function optimization (see also [5, 8]), although further research is required to measure and interpret the rate of specific metabolic pathways in an activation-dependent manner. In agreement with previous works, our model outcomes support a lactate transfer from neurons to astrocytes [56, 57, 60]. We found that the contribution of this lactate shuttle is very small, and occurs on top of neuronal and astrocytic glucose uptakes which are similar to each other. Interestingly, recent experimental findings showed higher glucose uptake in neurons relative to astrocytes [61, 62], which suggests that astrocytic energy requirements are met by substrates other than blood-derived glucose. Glycogen is one major candidate in providing substrates for astrocytic metabolism, as K^+ uptake in astrocytes is probably fueled by glycogenolysis [18, 63]. Interpretation of studies reporting predominantly astrocytic [64, 65] glucose uptake requires taking into account the impact of glycogen metabolism. Indeed, increased astrocytic glucose uptake observed in anesthesized animals [65]

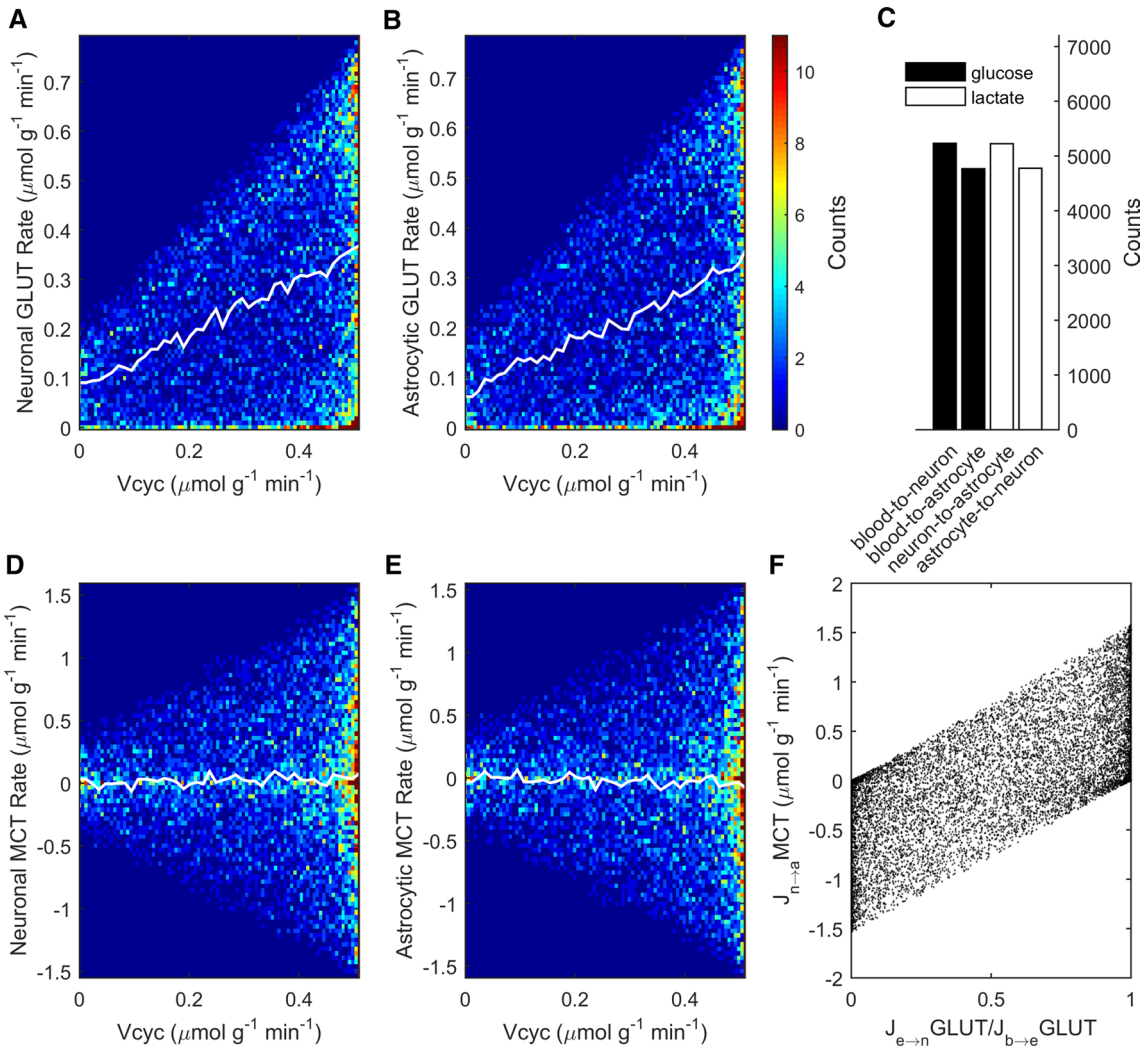

Fig. 4 Model outcomes for cellular glucose uptake and lactate shuttle. Simulated glucose uptake by **a** neuronal and **b** astrocytic GLUTs and concomitant lactate transport by **d** neuronal and **e** astrocytic MCTs. On average, glucose is taken up almost equally by neurons and astrocytes and intercellular lactate transfer is negligible across all activation levels. However, feasible solutions include extreme cases with one cell type taking up all glucose and the other relying exclusively on shuttled lactate. **c** The number of solutions supporting predominant neuronal glucose uptake and lactate release are slightly more numerous than solutions supporting the opposite. **f** The direction and magnitude of cell-to-cell lactate shuttle is directly controlled by the cellular uptake of glucose. Note that in order to compare the GLUT and MCT fluxes in terms of glucose equivalents, the MCT flux has to be divided by two. *Color plots* have been obtained as in Fig. 3. Note that the upper bound of the abscissa in panels **a, b, d, e** is at $Vcyc = Vcyc^0 = 0.51$ μm ol g^{-1} min−1 (awake value). (Color figure online)

or tissue slices [64] might reflect inactive glycogenolysis due to anesthesia or tissue glycogen depletion, respectively [66]. Furthermore, the use of the glucose analogues used in the studies that have reported higher astrocytic versus neuronal glucose uptake [64, 65] has been criticized based on transport kinetic analysis [67]. Finally, glucose utilization in astrocytes may be biased in the ^{13}C-MRS studies of anesthesized animals due to anesthesia-induced decrease in glycogen degradation and/or increase in glycogen synthesis. Unfortunately, glycogen metabolism cannot be incorporated into mass-balance models like the present one, unless ad-hoc constraints about the rate of glycogenolysis (currently unknown) are introduced.

One main limitation of the present FBA-based model is that metabolism can be studied only under steady-state conditions. Theoretical investigations about the transient metabolic processes (e.g., glycogenolysis) occurring in response to physiological stimulation on top of the awake condition require the development of kinetic models [60, 68]. This is especially relevant in the short-term response of the cortical tissue to stimulation, which is confined to tens of seconds/few minutes before a new, activated steady-state is eventually established [69, 70]. Another potential limitation is that we assumed a fixed stoichiometry for ionic currents induced by glutamatergic signaling across all activity levels, from isoelectric to awake conditions. In particular, the

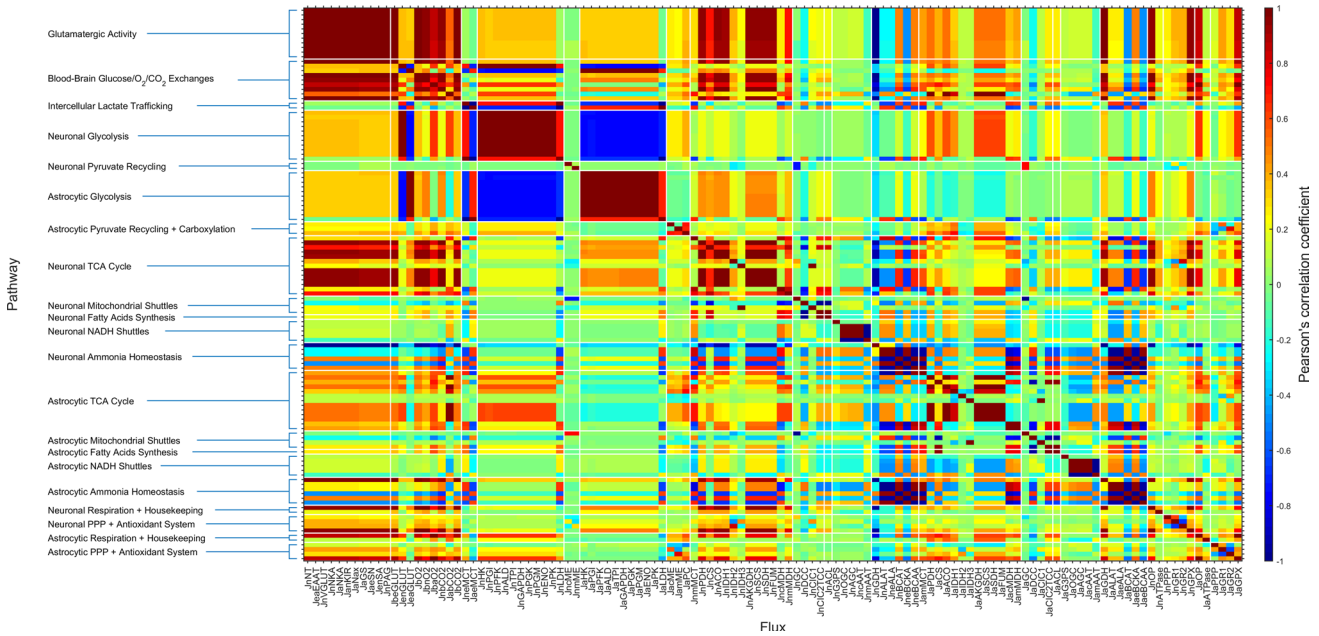

Fig. 5 Spread matrix of model solutions. Flux names are reported at the *bottom*, while grouped metabolic pathways are reported *sideways*. There is strong correlation between the reactions within the "glutamatergic activity" group as well as between this group and metabolic pathways (glycolysis, TCA cycle, respiration). As expected, pathways in the "ammonia homeostasis" group (including glutamate dehydrogenase-catalyzed reaction) exhibit opposite correlations in neurons and astrocytes. Cellular glycolysis and TCA cycle also form correlated groups. Noticeably, neuronal glycolysis is more correlated with astrocytic rather than neuronal TCA cycle, and vice versa. The spread matrix has been determined by computing the Pearson's correlation coefficient between each pair of reactions

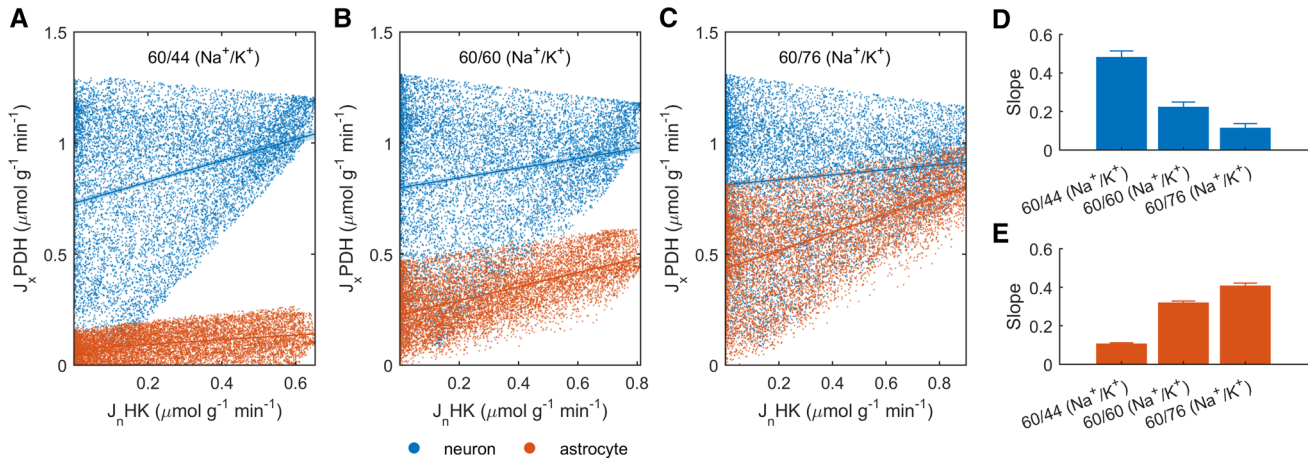

Fig. 6 Dependence of neuronal glycolysis and astrocytic glycolysis/TCA cycle on the Na^+/K^+ fluxes ratio. In neurons, the rate of HK, i.e. the enzyme commiting glucose to cellular glycolysis, is positively correlated with the rate of PDH, i.e. the enzyme channeling the product of glycolytic pathway pyruvate to cellular TCA cycle. However, this positive correlation decreases with increasing departures in Na^+ influx/K^+ efflux ratio (due to neuronal activity) above the 3/2 ratio underlying the activity of NKA, from 60/44 (**a**) to 60/60 (**b**) and beyond to 60/76 (**c**). Concomitantly, when voltage/ligand-gated fluxes are above the 3/2 Na^+/K^+ NKA ratio, neuronal HK becomes more and more correlated with astrocytic PDH, reflecting the fact that excess K^+ stimulates astrocytic activation and oxidative metabolism. Note that while the Na^+ influx/K^+ efflux ratio decreases, neuronally released K^+ increases because Na^+ influx is kept constant. **d, e** Summary of the slope of the linear curves fitting the simulated data. *Error bars* are determined by calculating the confidence intervals in each data plot with $p < 0.001$

quantitative relation between synaptic and spiking activity might produce dynamic ion movements across neurons and astrocytes in an activity-dependent manner, although such non-linear behavior is likely to be of relevance only at high physiological activity (i.e. under intense stimulation) [2]. Furthermore, it should be noted that the stoichiometry of 63 Na^+ entering and 58 K^+ exiting neurons per glutamate released comes from the assumption of a direct quantitative

link between glutamatergic neurotransmission and voltage/ligand-gated ionic currents. In fact, other mechanisms may indirectly concur to define such stoichiometry. For example, part of the inward neuronal Na^+ current can be carried by Ca^{2+} through the action of Na^+/Ca^{2+} exchanger [16]. Nonetheless, our model provides a theoretical framework to test various hypotheses about the relevance of specific metabolic pathways. For example, targeted enzyme deletions might be used to identify reaction/transport processes that are involved and/or essential in order to reproduce or support a certain experimental result. In this respect, a preliminary implication of our results is that under awake conditions glutamate dehydrogenase (GDH) appears to be necessary for neurotransmission (Online Resource 10 Panel F and Online Resource 15 Panel F). Indeed, glutamate-glutamine cycle entails concurrent maintenance of ammonia homeostasis in neurons and astrocytes, which requires GDH regardless of the identity of the associated amino acid shuttle [71]. Our results support the notion that GDH-catalyzed reaction runs in opposite direction in these cell types, aminating α-ketoglutarate in neurons and deaminating glutamate in astrocytes, thereby removing (in neurons) or providing (in astrocytes) ammonia for the conversion between glutamine and glutamate. However, other mechanisms have been proposed to support ammonia homeostasis in brain, which have not been implemented in the present model and may lessen the requirement for GDH, including diffusion of ammonia as gaseous NH_3 or the purine nucleotide cycle [71].

An interesting possibility for future research could be the incorporation of the stoichiometry between Na^+ and K^+ ionic fluxes and neuronal glutamate release that we report here into larger models of brain metabolism. Indeed, the set of reactions in our model is comparable to some previously published models (e.g., [8]) but much smaller than others (e.g., [9, 12]). Our approach to limit the analysis to the major pathways involved in glutamatergic signaling is equivalent to have assumed that the remaining parts of the metabolic network (not included in the present model) simply adapt to maintain the homeostasis of the metabolic species we considered. Extending large-scale metabolic models of brain metabolism with the information that we have found in the present study may allow to examine the effect of these additional metabolic pathways on the ionic movements underlying neurotransmission, and vice versa.

In conclusion, we have developed a mass-balance model of compartmentalized brain energy metabolism to examine the functional mechanisms underlying the metabolic relationships between neurons and astrocytes. Our analysis allowed the determination of a simple stoichiometric relation between activity-dependent ion and transmitter homeostasis in neurons (63/58 Na^+ influx/K^+ efflux per glutamate released). Based on experimental ^{13}C-NMR spectroscopy data obtained in rat brain we found that such ratio must be close to 1:1, thereby departing from the the 3/2 Na^+/K^+ ratio underlying NKA activity moving Na^+ and K^+ in the opposite direction to re-establish ion homeostasis. Thus, stoichiometry alone proved successful in reproducing experimental observations of activity-induced stimulation of astrocytes. These results support the idea [26] that the excess K^+ mechanism may constitute the basis for astrocytic activation in response to neuronal activity and corresponding neuron-astrocyte functional and metabolic interactions, a phenomenon that should not be neglected in studies aiming at investigating the contribution of these glial cells in brain energetics.

Acknowledgments The authors thank Dr. Markus Triska (TU Wien, Austria) and Dr. Jan Wielemaker (University of Amsterdam, The Netherlands) for their helpful comments and suggestions.

Funding This study is part of a project that has received funding from the European Union's Horizon 2020 research and innovation programme under the Marie Sklodowska-Curie Grant Agreement No. 701635. The content is solely the responsibility of the authors and does not necessarily represent the official views of the European Union.

Compliance with Ethical Standards

Conflict of Interest The authors have declared that no competing interests exist.

References

1. Harris JJ, Jolivet R, Attwell D (2012) Synaptic energy use and supply. Neuron 75:762–777
2. DiNuzzo M, Giove F (2012) Activity-dependent energy budget for neocortical signaling: effect of short-term synaptic plasticity on the energy expended by spiking and synaptic activity. J Neurosci Res 90:2094–2102
3. Mangia S, DiNuzzo M, Giove F, Carruthers A, Simpson IA, Vannucci SJ (2011) Response to 'comment on recent modeling studies of astrocyte-neuron metabolic interactions': much ado about nothing. J Cereb Blood Flow Metab 31:1346–1353
4. Sertbas M, Ulgen K, Cakir T (2014) Systematic analysis of transcription-level effects of neurodegenerative diseases on human brain metabolism by a newly reconstructed brain-specific metabolic network. FEBS Open Biol 4:542–553
5. Calvetti D, Somersalo E (2012) Menage a trois: the role of neurotransmitters in the energy metabolism of astrocytes, glutamatergic, and GABAergic neurons. J Cereb Blood Flow Metab 32:1472–1483
6. Massucci FA, DiNuzzo M, Giove F, Maraviglia B, Castillo IP, Marinari E, De Martino A (2013) Energy metabolism and glutamate-glutamine cycle in the brain: a stoichiometric modeling perspective. BMC Syst Biol 7:103

7. Calvetti D, Somersalo E (2013) Quantitative in silico analysis of neurotransmitter pathways under steady state conditions. Frontiers in endocrinology 4:137
8. Occhipinti R, Somersalo E, Calvetti D (2008) Astrocytes as the glucose shunt for glutamatergic neurons at high activity: an in silico study. J Neurophysiol 101:2528–2538
9. Cakir T, Alsan S, Saybasili H, Akin A, Ulgen KO (2007) Reconstruction and flux analysis of coupling between metabolic pathways of astrocytes and neurons: application to cerebral hypoxia. Theor Biol Med Model 4:48
10. Chatziioannou A, Palaiologos G, Kolisis FN (2003) Metabolic flux analysis as a tool for the elucidation of the metabolism of neurotransmitter glutamate. Metab Eng 5:201–210
11. Calvetti D, Somersalo E (2011) Dynamic activation model for a glutamatergic neurovascular unit. J Theor Biol 274:12–29
12. Lewis NE, Schramm G, Bordbar A, Schellenberger J, Andersen MP, Cheng JK, Patel N, Yee A, Lewis RA, Eils R, Konig R, Palsson BO (2010) Large-scale in silico modeling of metabolic interactions between cell types in the human brain. Nat Biotechnol 28:1279–1285
13. Vazquez A (2013) Metabolic states following accumulation of intracellular aggregates: implications for neurodegenerative diseases. PLoS One 8:e63822
14. Vereninov IA, Yurinskaya VE, Model MA, Lang F, Vereninov AA (2014) Computation of pump-leak flux balance in animal cells. Cell Physiol Biochem 34:1812–1823
15. Hertz L, Peng L, Dienel GA (2007) Energy metabolism in astrocytes: high rate of oxidative metabolism and spatiotemporal dependence on glycolysis/glycogenolysis. J Cereb Blood Flow Metab 27:219–249
16. Attwell D, Laughlin SB (2001) An energy budget for signaling in the grey matter of the brain. J Cereb Blood Flow Metab 21:1133–1145
17. Howarth C, Gleeson P, Attwell D (2012) Updated energy budgets for neural computation in the neocortex and cerebellum. J Cereb Blood Flow Metab 32:1222–1232
18. DiNuzzo M, Mangia S, Maraviglia B, Giove F (2012) The role of astrocytic glycogen in supporting the energetics of neuronal activity. Neurochem Res 37:2432–2438
19. Ruminot I, Gutierrez R, Pena-Munzenmayer G, Anazco C, Sotelo-Hitschfeld T, Lerchundi R, Niemeyer MI, Shull GE, Barros LF (2011) NBCe1 mediates the acute stimulation of astrocytic glycolysis by extracellular K^+. J Neurosci 31:14264–14271
20. Bittner CX, Valdebenito R, Ruminot I, Loaiza A, Larenas V, Sotelo-Hitschfeld T, Moldenhauer H, San Martin A, Gutierrez R, Zambrano M, Barros LF (2011) Fast and reversible stimulation of astrocytic glycolysis by K^+ and a delayed and persistent effect of glutamate. J Neurosci 31:4709–4713
21. Dienel GA, Cruz NF (2004) Nutrition during brain activation: does cell-to-cell lactate shuttling contribute significantly to sweet and sour food for thought? Neurochem Int 45:321–351
22. Hertz L, Swanson RA, Newman GC, Marrif H, Juurlink BH, Peng L (1998) Can experimental conditions explain the discrepancy over glutamate stimulation of aerobic glycolysis? Dev Neurosci 20:339–347
23. Peng L, Swanson RA, Hertz L (2001) Effects of L-glutamate, D-aspartate, and monensin on glycolytic and oxidative glucose metabolism in mouse astrocyte cultures: further evidence that glutamate uptake is metabolically driven by oxidative metabolism. Neurochem Int 38:437–443
24. Diamond JS, Jahr CE (2000) Synaptically released glutamate does not overwhelm transporters on hippocampal astrocytes during high-frequency stimulation. J Neurophysiol 83:2835–2843
25. DiNuzzo M, Mangia S, Maraviglia B, Giove F (2014) Physiological bases of the K^+ and the glutamate/GABA hypotheses of epilepsy. Epilepsy Res 108:995–1012
26. Hertz L, Xu J, Song D, Yan E, Gu L, Peng L (2013) Astrocytic and neuronal accumulation of elevated extracellular K(+) with a 2/3 K(+)/Na(+) flux ratio-consequences for energy metabolism, osmolarity and higher brain function. Front Comput Neurosci 7:114
27. Moujahid A, d'Anjou A (2012) Metabolic efficiency with fast spiking in the squid axon. Front Comput Neurosci 6:95
28. Hajek I, Subbarao KV, Hertz L (1996) Acute and chronic effects of potassium and noradrenaline on Na^+, K^+-ATPase activity in cultured mouse neurons and astrocytes. Neurochem Int 28:335–342
29. Honegger P, Pardo B (1999) Separate neuronal and glial Na^+, K^+-ATPase isoforms regulate glucose utilization in response to membrane depolarization and elevated extracellular potassium. J Cereb Blood Flow Metab 19:1051–1059
30. Grisar T, Frere JM, Franck G (1979) Effect of K^+ ions on kinetic properties of the (Na^+, K^+)-ATPase (EC 3.6.1.3) of bulk isolated glial cells, perikarya and synaptosomes from rabbit brain cortex. Brain Res 165:87–103
31. Sibson NR, Shen J, Mason GF, Rothman DL, Behar KL, Shulman RG (1998) Functional energy metabolism: in vivo ^{13}C-NMR spectroscopy evidence for coupling of cerebral glucose consumption and glutamatergic neuronalactivity. Dev Neurosci 20:321–330
32. Oz G, Berkich DA, Henry P-G, Xu Y, LaNoue K, Hutson SM, Gruetter R (2004) Neuroglial metabolism in the awake rat brain: CO_2 fixation increases with brain activity. J Neurosci 24:11273–11279
33. Hyder F, Fulbright RK, Shulman RG, Rothman DL (2013) Glutamatergic function in the resting awake human brain is supported by uniformly high oxidative energy. J Cereb Blood Flow Metab 33:339–347
34. Harris JJ, Attwell D (2012) The energetics of CNS white matter. J Neurosci 32:356–371
35. Lennie P (2003) The cost of cortical computation. Curr Biol 13:493–497
36. Holzbaur C (1995) OFAI CLP(Q, R), Manual, Edition 1.3.3. Technical Report TR-95-09. In. Austrian Research Institute for Artificial Intelligence, Vienna
37. Haralick RM, L. EG (1980) Increasing tree search efficiency for constraint satisfaction problems. Artif Intell 14:263–313
38. Riveros N, Fiedler J, Lagos N, Munoz C, Orrego F (1986) Glutamate in rat brain cortex synaptic vesicles: influence of the vesicle isolation procedure. Brain Res 386:405–408
39. Burger PM, Mehl E, Cameron PL, Maycox PR, Baumert M, Lottspeich F, De Camilli P, Jahn R (1989) Synaptic vesicles immunoisolated from rat cerebral cortex contain high levels of glutamate. Neuron 3:715–720
40. Zampighi GA, Fisher RS (1997) Polyhedral protein cages encase synaptic vesicles and participate in their attachment to the active zone. J Struct Biol 119:347–359
41. Takamori S, Holt M, Stenius K, Lemke EA, Gronborg M, Riedel D, Urlaub H, Schenck S, Brugger B, Ringler P, Muller SA, Rammner B, Grater F, Hub JS, De Groot BL, Mieskes G, Moriyama Y, Klingauf J, Grubmuller H, Heuser J, Wieland F, Jahn R (2006) Molecular anatomy of a trafficking organelle. Cell 127:831–846
42. Sibson NR, Dhankhar A, Mason GF, Rothman DL, Behar KL, Shulman RG (1998) Stoichiometric coupling of brain glucose metabolism and glutamatergic neuronal activity. Proc Natl Acad Sci USA 95:316–321
43. Patel AB, de Graaf RA, Mason GF, Rothman DL, Shulman RG, Behar KL (2005) The contribution of GABA to glutamate/glutamine cycling and energy metabolism in the rat cortex in vivo. Proc Natl Acad Sci USA 102:5588–5593
44. Choi IY, Lei H, Gruetter R (2002) Effect of deep pentobarbital anesthesia on neurotransmitter metabolism in vivo: on the

correlation of total glucose consumption with glutamatergic action. J Cereb Blood Flow Metab 22:1343–1351
45. Duarte JM, Lanz B, Gruetter R (2011) Compartmentalized cerebral metabolism of [1,6-(13)C]glucose determined by in vivo (13) C NMR spectroscopy at 14.1 T. Front Neuroenergetics 3:3
46. Patel AB, de Graaf RA, Mason GF, Kanamatsu T, Rothman DL, Shulman RG, Behar KL (2004) Glutamatergic neurotransmission and neuronal glucose oxidation are coupled during intense neuronal activation. J Cereb Blood Flow Metab 24:972–985
47. Patel AB, Chowdhury GM, de Graaf RA, Rothman DL, Shulman RG, Behar KL (2005) Cerebral pyruvate carboxylase flux is unaltered during bicuculline-seizures. J Neurosci Res 79:128–138
48. Serres S, Raffard G, Franconi JM, Merle M (2008) Close coupling between astrocytic and neuronal metabolisms to fulfill anaplerotic and energy needs in the rat brain. J Cereb Blood Flow Metab 28:712–724
49. van Eijsden P, Behar KL, Mason GF, Braun KP, de Graaf RA (2010) In vivo neurochemical profiling of rat brain by 1H-[13C] NMR spectroscopy: cerebral energetics and glutamatergic/GABAergic neurotransmission. J Neurochem 112:24–33
50. Yang J, Shen J (2005) In vivo evidence for reduced cortical glutamate-glutamine cycling in rats treated with the antidepressant/antipanic drug phenelzine. Neuroscience 135:927–937
51. Chowdhury GM, Patel AB, Mason GF, Rothman DL, Behar KL (2007) Glutamatergic and GABAergic neurotransmitter cycling and energy metabolism in rat cerebral cortex during postnatal development. J Cereb Blood Flow Metab 27:1895–1907
52. de Graaf RA, Mason GF, Patel AB, Rothman DL, Behar KL (2004) Regional glucose metabolism and glutamatergic neurotransmission in rat brain in vivo. Proc Natl Acad Sci USA 101:12700–12705
53. Wang J, Jiang L, Jiang Y, Ma X, Chowdhury GM, Mason GF (2010) Regional metabolite levels and turnover in the awake rat brain under the influence of nicotine. J Neurochem 113:1447–1458
54. Hyder F, Patel AB, Gjedde A, Rothman DL, Behar KL, Shulman RG (2006) Neuronal-glial glucose oxidation and glutamatergic-GABAergic function. J Cereb Blood Flow Metab 26:865–877
55. Takahashi S, Izawa Y, Suzuki N (2012) Astroglial pentose phosphate pathway rates in response to high-glucose environments. ASN Neuro 4:AN20120002
56. Simpson IA, Carruthers A, Vannucci SJ (2007) Supply and demand in cerebral energy metabolism: the role of nutrient transporters. J Cereb Blood Flow Metab 27:1766–1791
57. Mangia S, Simpson IA, Vannucci SJ, Carruthers A (2009) The in vivo neuron-to-astrocyte lactate shuttle in human brain: evidence from modeling of measured lactate levels during visual stimulation. J Neurochem 109(Suppl 1):55–62
58. Dienel GA (2013) Astrocytic energetics during excitatory neurotransmission: what are contributions of glutamate oxidation and glycolysis? Neurochem Int 63:244–258
59. McKenna MC (2013) Glutamate pays its own way in astrocytes. Front Endocrinol 4:191
60. DiNuzzo M, Mangia S, Maraviglia B, Giove F (2010) Changes in glucose uptake rather than lactate shuttle take center stage in subserving neuroenergetics: evidence from mathematical modeling. J Cereb Blood Flow Metab 30:586–602
61. Patel AB, Lai JC, Chowdhury GM, Hyder F, Rothman DL, Shulman RG, Behar KL (2014) Direct evidence for activity-dependent glucose phosphorylation in neurons with implications for the astrocyte-to-neuron lactate shuttle. Proc Natl Acad Sci USA 111:5385–5390
62. Lundgaard I, Li B, Xie L, Kang H, Sanggaard S, Haswell JD, Sun W, Goldman S, Blekot S, Nielsen M, Takano T, Deane R, Nedergaard M (2015) Direct neuronal glucose uptake Heralds activity-dependent increases in cerebral metabolism. Nat Commun 6:6807
63. Xu J, Song D, Xue Z, Gu L, Hertz L, Peng L (2013) Requirement of glycogenolysis for uptake of increased extracellular K(+) in astrocytes: potential implications for K(+) homeostasis and glycogen usage in brain. Neurochem Res 38:472–485
64. Jakoby P, Schmidt E, Ruminot I, Gutierrez R, Barros LF, Deitmer JW (2013) Higher transport and metabolism of glucose in astrocytes compared with neurons: a multiphoton study of hippocampal and cerebellar tissue slices. Cereb Cortex 24:222–231
65. Chuquet J, Quilichini P, Nimchinsky EA, Buzsaki G (2010) Predominant enhancement of glucose uptake in astrocytes versus neurons during activation of the somatosensory cortex. J Neurosci 30:15298–15303
66. Takano T, He W, Han X, Wang F, Xu Q, Wang X, Oberheim Bush NA, Cruz N, Dienel GA, Nedergaard M (2014) Rapid manifestation of reactive astrogliosis in acute hippocampal brain slices. Glia 62:78–95
67. DiNuzzo M, Giove F, Maraviglia B, Mangia S (2013) Glucose metabolism down-regulates the uptake of 6-(*N*-(7-nitrobenz-2-oxa-1,3-diazol-4-yl)amino)-2-deoxyglucose (6-NBDG) mediated by glucose transporter 1 isoform (GLUT1): theory and simulations using the symmetric four-state carrier model. J Neurochem 125:236–246
68. DiNuzzo M, Mangia S, Maraviglia B, Giove F (2010) Glycogenolysis in astrocytes supports blood-borne glucose channeling not glycogen-derived lactate shuttling to neurons: evidence from mathematical modeling. J Cereb Blood Flow Metab 30:1895–1904
69. Mangia S, Tkac I, Gruetter R, Van de Moortele PF, Maraviglia B, Ugurbil K (2007) Sustained neuronal activation raises oxidative metabolism to a new steady-state level: evidence from 1H NMR spectroscopy in the human visual cortex. J Cereb Blood Flow Metab 27:1055–1063
70. Mangia S, Garreffa G, Bianciardi M, Giove F, Di Salle F, Maraviglia B (2003) The aerobic brain: lactate decrease at the onset of neural activity. Neuroscience 118:7–10
71. Rothman DL, De Feyter HM, Maciejewski PK, Behar KL (2012) Is there in vivo evidence for amino acid shuttles carrying ammonia from neurons to astrocytes? Neurochem Res 37:2597–2612